



## Green synthesis and characterization of magnetite ( $\text{Fe}_3\text{O}_4$ ) nanoparticles using leaf extract of *Alternanthera Philoxeroides* for environmental applications

Md. Anwarul Kabir Bhuiya<sup>\*</sup>, Md Abdur Rahman<sup>1</sup>, Md Shoeb<sup>1</sup> Md. Asadul Islam<sup>1</sup>, Sajib Madbar<sup>1</sup>, Muniat Niva<sup>1</sup>, Md. Saiful Islam<sup>1</sup>, Samia Tabassum<sup>2</sup>

<sup>1</sup>*Department of Materials Science and Engineering, Faculty of Engineering, University of Rajshahi, Bangladesh*

<sup>2</sup>*Senior Scientific Officer, Institute of Fuel Research and Development (IFRD), BCSIR, Dhaka, Bangladesh*

**Key words:** Magnetite nanoparticles ( $\text{Fe}_3\text{O}_4$ NPs), Green synthesis, *Alternanthera Philoxeroides*, UV- visible Spectroscopy, TGA, DTA, VSM and FTIR

<http://dx.doi.org/10.12692/ijb/22.6.123-132>

Article published on June 12, 2023

### Abstract

Iron oxide nanoparticles, notably magnetite ( $\text{Fe}_3\text{O}_4$ ), have become widely used and a key topic of research due to their superparamagnetism and distinctive features. As a result, scientists are diligently looking into new uses for these nanoparticles. The choice and use of synthesis techniques are important variables that might affect the size and characteristics of the nanoparticles (NPs). The use of harmful compounds that are absorbed on the surface of the nanoparticles has been linked to a number of negative impacts of chemical production processes. The Green synthesis of nanoparticles has evolved as an eco-friendly method in response to environmental concerns, giving researchers the chance to internationally investigate the potential of various herbs for nanoparticle synthesis. The aqueous extract of *Alternanthera Philoxeroides* leaves and the precursors ferric chloride anhydrous ( $\text{FeCl}_3$  anhydrous) and ferrous chloride tetrahydrate ( $\text{FeCl}_2 \cdot 4\text{H}_2\text{O}$ ) are used in this study to demonstrate a green synthesis approach for manufacturing magnetite nanoparticles. Thermogravimetric analysis (TGA), Fourier transform infrared spectroscopy (FTIR), vibrating-sample magnetometer (VSM), and UV-visible spectroscopy were used to evaluate the produced FeNPs. The presence of functional groups including (-OH), (C-H), and (-NH) was detected in the FTIR findings, showing that organic compounds had been coated on the FeNPs. A maximum absorption peak was detected in the ultraviolet-visible spectra of the aqueous media containing iron nanoparticles at about 330 nm. The magnetic characteristics of the produced FeNPs were verified by VSM testing. Numerous uses for these nanoparticles exist, such as waste water treatment, energy production, and others.

**\* Corresponding Author:** Dr. Md. Anwarul Kabir Bhuiya ✉ [mkabir@ru.ac.bd](mailto:mkabir@ru.ac.bd).

## Introduction

Nanoparticles have seen an increase in demand in recent years, due to their use in various fields, including health, catalysis, energy, and drug delivery systems (Nam *et al.*, 2009; Li *et al.*, 2011). The physical, chemical, optical, and electrical properties of these nanomaterials are significantly influenced by the size, shape, and surface morphology of the nanoparticles. Various techniques, including physical vapor deposition, chemical vapor deposition, the sol-gel method, co-precipitation method, ultrasonic method, electrochemical synthesis, and chemical reduction of metallic ions, are used to create metallic nanoparticles (Horwat *et al.*, 2011; Sobhani *et al.*, 2011; Starowicz *et al.*, 2006). These Syntheses frequently involve toxic, expensive, and unsustainable substances. Due to the simplicity of synthesis, environmental friendliness, and increased stability of nanoparticles, green synthesis approaches based on fungus, microbes, plant and peel extracts are currently being investigated (Balaji *et al.*, 2009; Kumar *et al.*, 2011; Sukirtha *et al.*, 2012).

Because of their high saturation magnetization,  $\text{Fe}_3\text{O}_4$  MNPs are simple to magnetically separate in an external magnetic field (Mohamed *et al.*, 2017). Several studies have been done on the synthesis of MNPs using a variety of reducing agents, including hydrazine (Hou *et al.*, 2005). Dimethyl formamide (Jian *et al.*, 2006). Sodium borohydride (Cain *et al.*, 1996). Carbon monoxide (Mondal *et al.*, 2004) and others. The biocompatibility of MNPs is hampered by these highly reactive reducing agents, which also have negative environmental impacts. As a result, there are only a few bio-medical uses for chemically reduced MNPs. MNPs must be strictly biocompatible in order to be used in biomedical applications. Several research using plant extracts to synthesize  $\text{Fe}_3\text{O}_4$ -NPs have been successful. For instance, *Artemisia annua* fruit extract (Basavegowda *et al.*, 2014). *Perilla frutescens* leaf extract (Basavegowda *et al.*, 2014). *Tridax procumbens* (Senthil *et al.*, 2012). *Caricaya* papaya extract (Latha *et al.*, 2014). Plantain peel extract (Venkateswarlu *et al.*, 2013). Grape proanthocyanidin seed extract (Narayanan *et al.*,

2012). In the leaf extract, there are a number of polyphenols and acidic compounds available. These Polyphenols from the extract form complexes with metal ions and show both reducing and capping behavior for NPs Senthil *et al.*, 2012. Also, these polyphenolic compounds are biodegradable, nontoxic, and water-soluble at room temperature, which proves that green leaf extract as an effective reducing agent compared to others (Latha *et al.*, 2014). According to the literature analysis, no specific studies have been conducted on the synthesis of  $\text{Fe}_3\text{O}_4$ -NPs using the alligator weed *Alternanthera Philoxeroides*, which encourages and pushes us to work on this. We have developed a modified green synthesis method to prepare  $\text{Fe}_3\text{O}_4$ -NPs using green *Alternanthera Philoxeroides* extract as a reducing agent, a novel environmentally friendly technique for producing  $\text{Fe}_3\text{O}_4$ -NPs is suggested in this study.

## Materials and methods

### Materials

Iron (II) chloride tetrahydrate ( $\text{FeCl}_2 \cdot 4\text{H}_2\text{O} \geq 99\%$ ) and iron (III) chloride hexahydrate ( $\text{FeCl}_3 \cdot 6\text{H}_2\text{O}$ , 97 %) were purchased from Sigma-Aldrich. Sodium hydroxide (NaOH) was obtained from R&M Chemicals. All the chemicals were used without further purification. All the aqueous solutions were prepared by deionized water purchased from Rimso Bangladesh.

### Sample collection

The fresh leaf of *Alternanthera Philoxeroides* was collected from the Botanical garden pond side at the University of Rajshahi campus. The collected leaves were washed thoroughly for multiple times and immersed in a deionized water for 2 hrs. The leaves of *Alternanthera Philoxeroides* (AP) were cut into small pieces and then again washed with deionized water. After that, The leaves were dried at room temperature and cut into small size.

### Preparation of leaf extract

An extract was prepared using 20 grams of these leaves in a 500 mL beaker, which contained 200 mL of distilled water. The mixture was then heated and

boiled at 60°C for one hour. During the boiling process, the solution's color transformed from watery to yellowish-brown. After boiling, the mixture was allowed to cool down to room temperature. To separate the leaves from the extract, the solution was filtered using "Double Rings" filter paper. The resulting filtered extract was then stored at 4°C until it was ready to be used for further experimentation or analysis.

#### *Green Synthesis of Alternanthera Philoxeroides leaf Fe<sub>3</sub>O<sub>4</sub>-NPs*

The synthesis of magnetite (Fe<sub>3</sub>O<sub>4</sub>) nanoparticles is carried out using the following method: A 1:2M ratio of ferrous chloride tetrahydrate (FeCl<sub>2</sub>·4H<sub>2</sub>O) and ferric chloride anhydrous (FeCl<sub>3</sub>) was dissolved in 100mL of distilled water. The solution was placed in a 250mL beaker and then heated to 80°C. During the process, mild stirring was applied using a magnetic stirrer. After 20 minutes of the initial synthesis process, 50mL of Alternanthera Philoxeroides (AP) leaf extract was added gradually to the mixture. As a result of this addition, the mixture promptly changed its color to reddish-brown. Subsequently, the mixture was stirred continuously for 2 hours at a temperature of 60°C. Following the previous step, a 1M solution of NaOH (40mL) was added to the mixture at a controlled rate of 3 mL per minute. As a result of this addition, the reddish-brown mixture underwent a transformation and turned into a black-colored solution. The purpose of adding the NaOH solution was to facilitate the uniform precipitation of magnetite. After adding the NaOH solution, the black solution was continuously stirred for approximately 30 minutes at 60°C. This additional stirring time allowed the reaction to complete, leading to the formation of the final black precipitate, which consists of the magnetite nanoparticles.

The next step involved in the process was centrifugation, which was performed at 5000 rpm for 6 minutes, and this step was repeated 6-7 times. In the second part, the magnetite nanoparticles were purified and then subjected to drying in a vacuum oven overnight at a temperature of 70°C. This drying

process transformed the nanoparticles into a fine powder. To achieve the fine powder consistency, the dried nanoparticles were crushed using a mortar.

#### *Characterization*

A PG Instruments T60 UV-Visible spectrophotometer was used to measure the absorbance. The presence of the biomolecules needed for the synthesis of Fe<sub>3</sub>O<sub>4</sub>-NPs was investigated using Fourier transform infrared (FT-IR) spectroscopy. Potassium bromide (KBr) was used to grind dried samples into pellets, which were then analyzed at 400–4000 cm<sup>-1</sup> wavelengths. Thermal stability is assessed using TGA and DTA analyses, and magnetic characteristics are assessed using a vibrating sample magnetometer.

#### **Result and discussion**

##### *Fourier Transform Infrared (FTIR) analysis of Fe<sub>3</sub>O<sub>4</sub>-NPs*

To determine the potential biomolecules involved in the reduction of iron ions and capping of the bio-reduced Fe<sub>3</sub>O<sub>4</sub>-NPs produced by the Alternanthera Philoxeroides extract, the FT-IR spectra were taken. To separate the Fe<sub>3</sub>O<sub>4</sub>-NPs from the proteins and other substances in the solution after the iron ions had fully undergone bio-reduction, the Alternanthera Philoxeroides leaf powder extract was centrifuged at 5000 rpm for 5–6 minutes for 6-7 times (Venkateswarlu *et al.*, 2014). The observed FTIR spectrum in Figure 3 showed distinct peaks at various wavenumbers. According to the peak at 3433 cm<sup>-1</sup>, which is caused by the stretching vibration of hydroxyl (-OH) groups, alcohols, phenols, or water molecules derived from AP's leaf extract are present. The sample contains C-H bonds, as evidenced by the signal at 2968 cm<sup>-1</sup>. The existence of heterocyclic chemicals like alkaloids or flavones is suggested by the peaks at -C-C-, -C-O-, and -C=C-, whereas the amide (I) bond peak is caused by proteins in the leaf-powder extract that serve as capping ligands for the nanoparticles. Indicated by a peak at 1634 cm<sup>-1</sup>, the presence of hydroxyl groups in the nanoparticle matrix is supported by the bending vibration of -OH groups in water molecules. The signal at 1384 cm<sup>-1</sup> denotes the existence of aromatic ring vibrations or

carboxylic acid groups (C=O stretching), which may have originated from bioactive chemicals in the leaf extract. Additionally, the peak at 1193  $\text{cm}^{-1}$  denotes C-O-C stretching vibrations, perhaps brought on by polyphenols or other organic compounds in the leaf extract, which play a crucial role in reducing and stabilizing MNPs. A peak at 1106  $\text{cm}^{-1}$  indicates the presence of C-N bonds, most likely originating from amino acids or proteins in the leaf extract, which helped to create and stabilize the nanoparticles.

Notably, peaks at 603  $\text{cm}^{-1}$  and 438  $\text{cm}^{-1}$ , which correspond to the stretching and bending vibrations of metal-oxygen (Fe-O) bonds, respectively, confirm the creation of magnetite ( $\text{Fe}_3\text{O}_4$ ) nanoparticles (Pham *et al.*, 2016). According to the FTIR study, the successful synthesis of MNPs utilizing an environmentally safe approach and AP leaf extract holds significant promise for a variety of uses in biotechnology, environmental remediation, and nanotechnology.

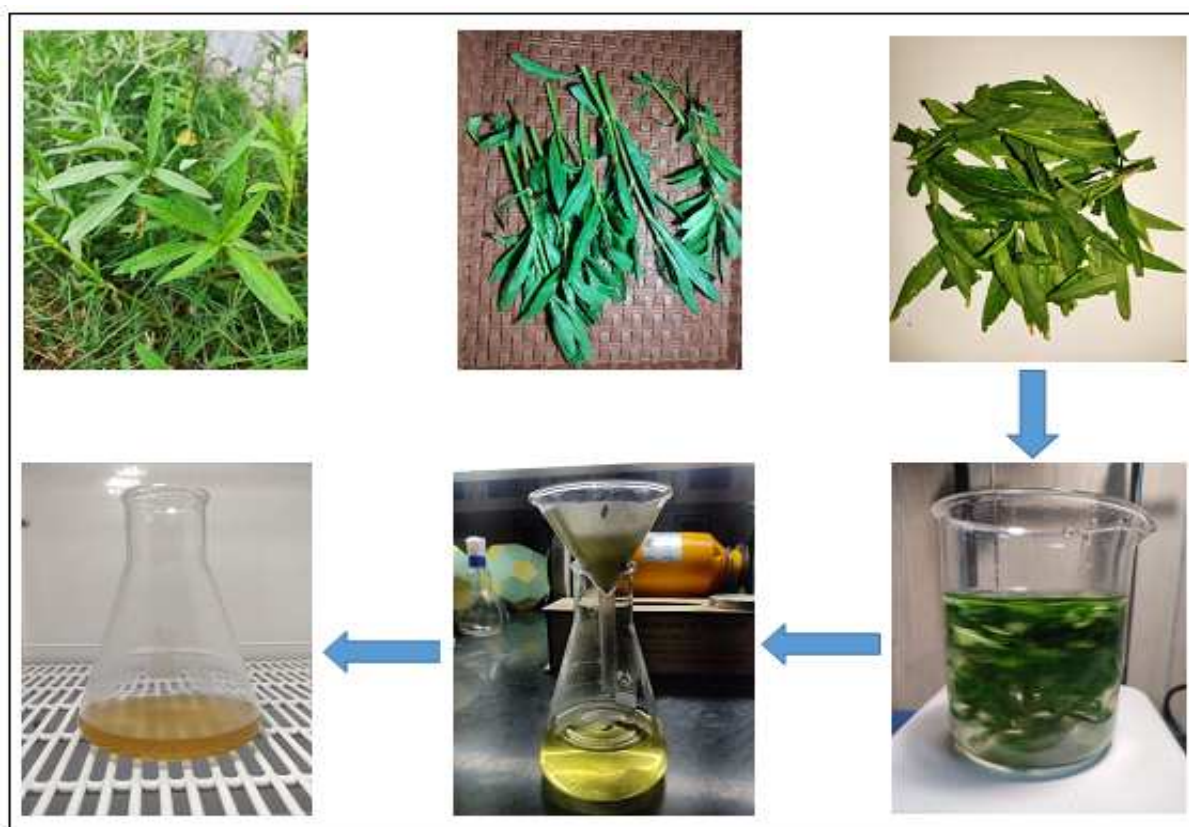


**Fig. 1.** Preparation of *Alternanthera Philoxeroides* Leaf extract.

#### *UV-visible spectroscopy*

In distilled water with a trace number of magnetite nanoparticles, a quartz cuvette was used to record the UV-Vis spectrum. At room temperature, the material was scanned over the 200–800 nm wavelength range. Figure 4 displays the UV-vis spectra of the two magnetite nanoparticles obtained by AP leaf. The appearance of a distinct absorption band at 330 nm supports the creation of  $\text{Fe}_3\text{O}_4$ -NPs, principally as a result of light absorption and scattering by these nanoparticles, according to an analysis of the absorbance of the  $\text{Fe}_3\text{O}_4$ -NPs solution using UV-Vis

spectroscopy (Ramesh *et al.*, 2018). For iron-based NPs, a continuous absorption band is frequently found in the 200–400 nm range (Ahmad *et al.*, 2009). This broad spectrum look most likely results from the interaction between iron salts and the phytochemicals found in leaf extracts (Bishnoi *et al.*, 2018). Similar UV-vis spectra for  $\text{Fe}_3\text{O}_4$ -NPs made from *Calliandra haematocephala* leaf extract and *Kappaphycus alvarezii* seaweed extract have previously been reported (Yew *et al.*, 2016; Sirdeshpande *et al.*, 2018). The development of largely unagglomerated nanosized particles is



indicated by the strong absorption band at 330 nm (Ahmad *et al.*, 2009). The lack of any hump spectra and the broadband appearance indicate that the size of the produced nanoparticles varies only little (Das *et al.*, 2020). Using a vibrating sample magnetometer

(VSM) at room temperature, magnetization measurements were made in order to examine the magnetic behavior of iron nanoparticles ( $\text{Fe}_3\text{O}_4$ -NPs) generated by Green.

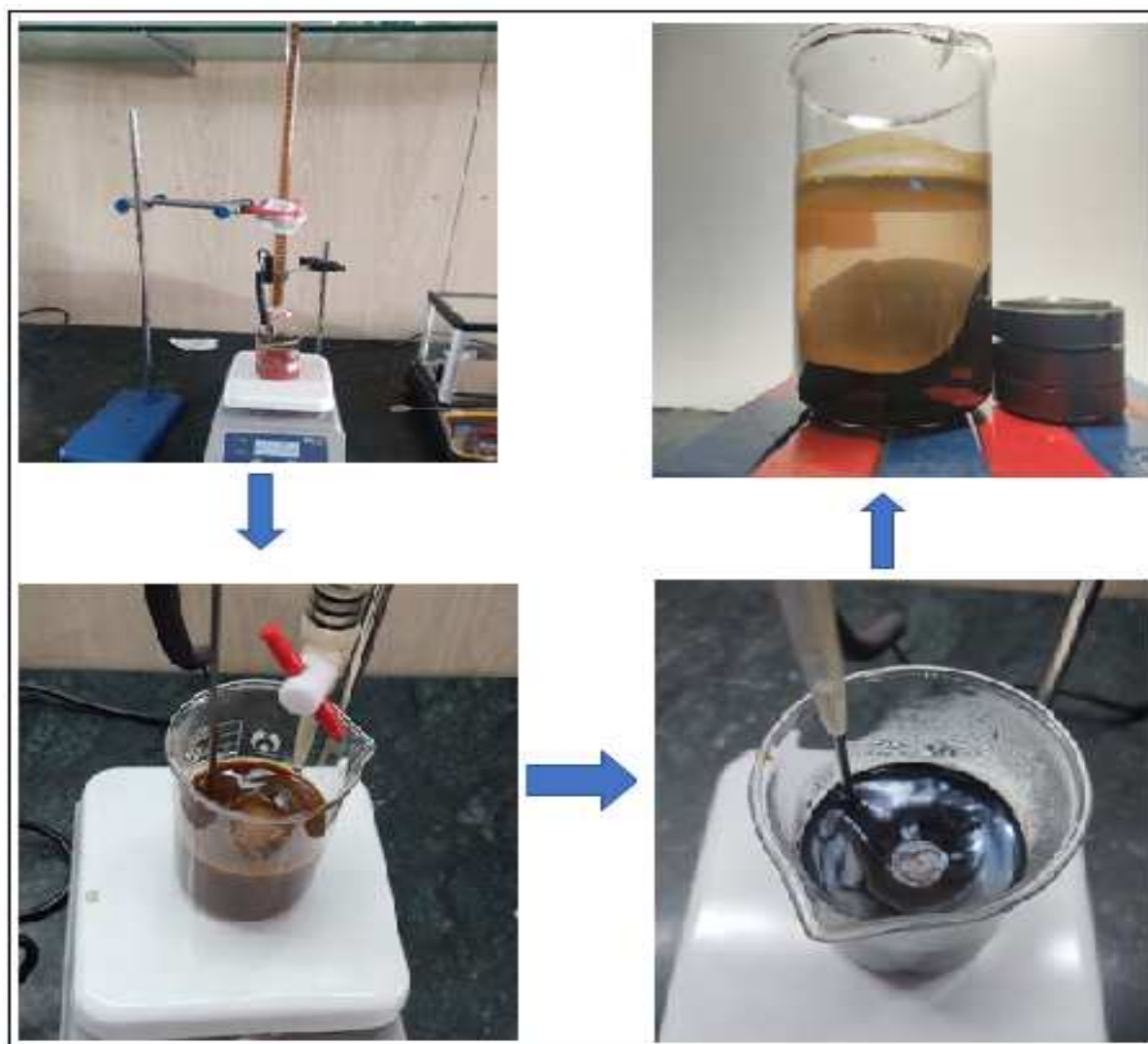


**Fig. 2.** Preparation of  $\text{Fe}_3\text{O}_4$  NPs.

The magnetization curve of the synthetic  $\text{Fe}_3\text{O}_4$ -NPs is shown in Figure 5, which also shows the magnetic response of magnetite  $\text{Fe}_3\text{O}_4$  nanoparticles at ambient temperature. Using AP leaf extract, the vibrating sample magnetometer (VSM) study was done to determine the magnetic characteristics of the produced magnetite nanoparticles (MNPs). Magnetic saturation ( $M_s$ ) = 14 emu/gm, remanent magnetization ( $M_r$ ) = 0.7 emu/gm, and coercivity ( $H_c$ ) = 10.6 Oe are the results of the hysteresis loop.

The maximum magnetization possible in the MNPs under the applied magnetic field is shown by the measured magnetic saturation ( $M_s$ ) of 14 emu/gm. The MNPs appear to have strong magnetic characteristics, which is beneficial for many applications in magnetic separation and targeted drug delivery systems, according to this high value. The residual magnetization that persists in the MNPs after the removal of the external magnetic field is indicated by the remanent magnetization ( $M_r$ ) value of 0.7 emu/gm.

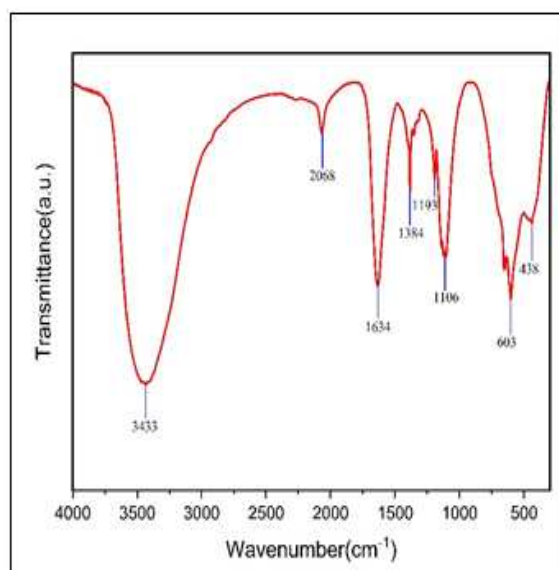


**Fig. 3.** FTIR Spectra of Fe<sub>3</sub>O<sub>4</sub>-NPs Powder.

The fact that this number is non-zero indicates that the synthesized MNPs have some magnetic retention, which adds to their stability and suggests that they might be used in long-term applications. The magnetic field intensity necessary to completely demagnetize the MNPs is represented by the coercivity ( $H_c$ ) value of 10.6 Oe. The MNPs are suitable for reversible magnetic applications, such as magnetic data storage and medication release, because their low coercivity value suggests that they can be readily magnetized and demagnetized (Pham *et al.*, 2016). A number of biomedical and environmental applications, including water filtration systems, magnetic hyperthermia for cancer therapy, and magnetic resonance imaging (MRI) contrast agents, are possible for the synthesized MNPs because of their combination of high magnetic saturation, significant remanent magnetization, and low coercivity (Akbarizadeh *et al.*, 2022).

#### *Thermo gravimetric analysis (TGA)*

By measuring changes in weight as a function of temperature, the Thermo gravimetric Analysis (TGA) method is a potent tool for understanding the thermal behavior of materials. TGA was used to examine the stability and thermal breakdown characteristics of Fe<sub>3</sub>O<sub>4</sub>-NPs that were produced using green synthesis. The first stage of deterioration took place during the first stage of TGA below 200°C, causing a weight loss of around 7.23%. This weight loss is a result of any

moisture or water that was still adsorbing on the Fe<sub>3</sub>O<sub>4</sub>-NPs' surface evaporating (Rami *et al.*, 2021).

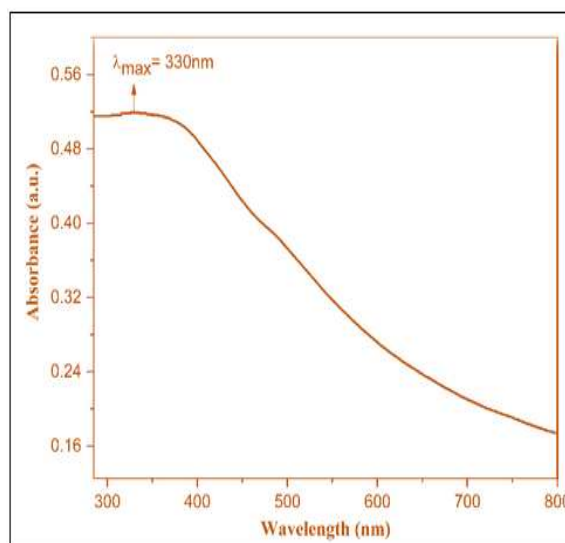


**Fig. 4.** UV-Vis absorption spectrum of Fe<sub>3</sub>O<sub>4</sub>-NPs.

This result supports the existence of water molecules in the nanoparticle structure, which is common for materials, particularly those created by biological synthesis. A weight loss of about 9.54% happened as the temperature increased in the second stage, which covered a range of roughly 200-400 °C.

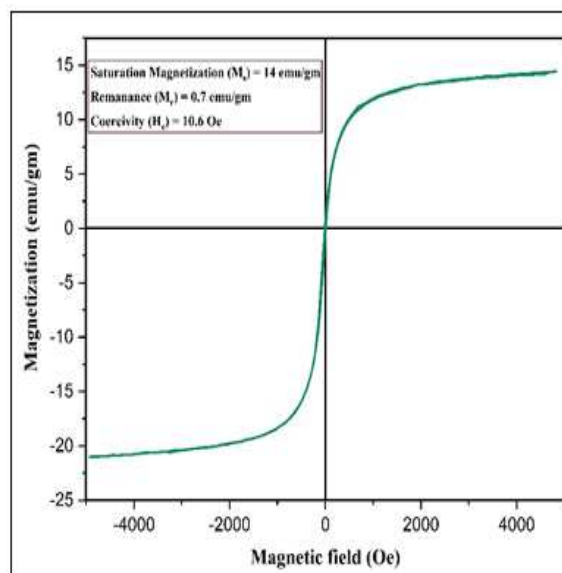


**Fig. 5.** VSM curve of Fe<sub>3</sub>O<sub>4</sub>-NPs.

This weight loss demonstrated the degradation of the organic materials found in the green-produced Fe<sub>3</sub>O<sub>4</sub>-NPs. These organic substances can be proteins, biomolecules, or other stabilizing elements employed in the creation of nanoparticles. The general structure and characteristics of the Fe<sub>3</sub>O<sub>4</sub>-NPs may vary as a

result of the breakdown of these organic components. Furthermore, a further weight loss of roughly 0.78% was noted at temperatures higher than 400 °C. The disintegration of the green-synthesised Fe<sub>3</sub>O<sub>4</sub>-NPs at higher temperatures was linked to this weight loss. As a result, the Fe<sub>3</sub>O<sub>4</sub> nanoparticles changed into FeO at this point. Since FeO is known to be substantially more stable than Fe<sub>3</sub>O<sub>4</sub>, the conversion of Fe<sub>3</sub>O<sub>4</sub> to FeO is interesting because it suggests a change in the thermal behavior of the nanoparticles (Bhuiyan *et al.*, 2020).

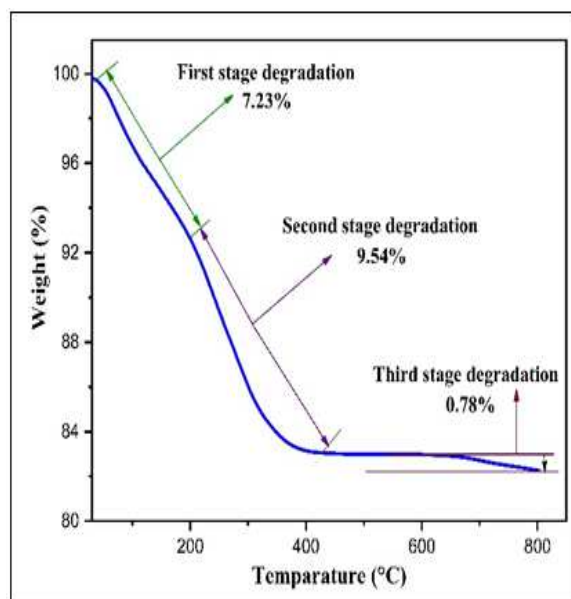


**Fig. 6.** TGA curve of Fe<sub>3</sub>O<sub>4</sub>-NPs.

#### Differential thermal analysis

Phase transitions, melting points, and other thermal events in materials where physical and chemical changes might occur are studied using the Differential.

Thermal Analysis (DTA) technique. Based on the direction of heat movement, these changes are classified as endothermic or exothermic. Endothermic peaks can be seen at the following locations in the DTA curves produced at a heating rate of 20°C/min: An endothermic peak was seen at 331 °C, indicating that heat was absorbed during a phase transition or structural change within the MNPs. In a similar manner, an endothermic peak was seen at 417 °C, confirming the degradation of organic matter and carbonaceous materials (Rajendrachari *et al.*, 2020).

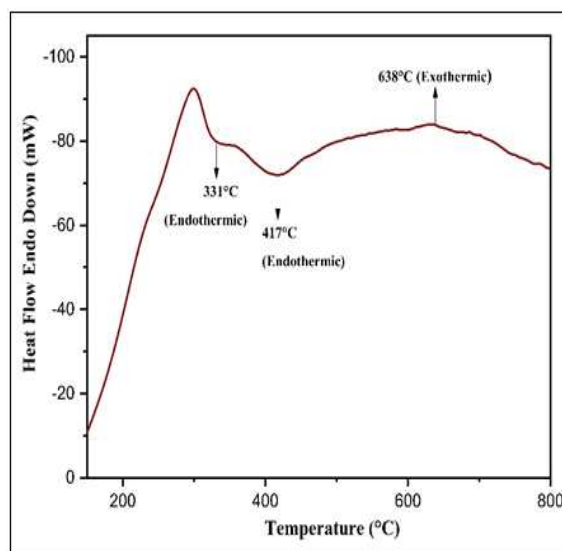


**Fig. 7.** DTA curve of Fe<sub>3</sub>O<sub>4</sub>-NPs.

The material undergoes a specific phase transition when Fe<sub>3</sub>O<sub>4</sub> (iron (II,III) oxide) changes to FeO (iron(II) oxide), which alters the crystal structure. The conversion of wüstite (FeO) from magnetite (Fe<sub>3</sub>O<sub>4</sub>) is known as this phase transition. Fe<sub>3</sub>O<sub>4</sub> is reduced exothermically to FeO in this mechanism. Iron (II,III) oxide Fe<sub>3</sub>O<sub>4</sub> loses oxygen atoms during this transition, which causes the iron ions to rearrange to create iron(II) oxide (FeO). Heat is released into the environment as a result of the liberation of energy caused by the release of oxygen and the rearranging of the iron ions. The release of heat during a phase transition, possibly involving the reduction of magnetite (Fe<sub>3</sub>O<sub>4</sub>) to FeO and the subsequent release of energy, was thus apparent when the temperature increased to 638°C, where an exothermic peak was visible. (Jalil *et al.*, 2017).

#### Conclusion

This study effectively established a bio-synthesis technique for manufacturing Fe<sub>3</sub>O<sub>4</sub>-NPs that is safe, non-toxic, and environmentally beneficial. The success in this area has created potential for the development of "greener" methods for producing optimal structural iron nanoparticles from mild starting materials. Due to the use of hazardous substances, conventional chemical and physical methods for creating nanoparticles are expensive and cause environmental issues. Contrarily, bio-inspired techniques have benefits like economic feasibility,

avoiding hazardous chemicals, and requiring less heat and energy. The green chemistry method used in the production of Fe<sub>3</sub>O<sub>4</sub>-NP has a number of advantages, including easy scaling and financial feasibility. Alligator weed or broadleaf carpet grass, also known as *Alternanthera Philoxeroides*, is a particularly invasive type of aquatic plant. In our country, this plant frequently ends up as trash in ponds and other bodies of water and is occasionally fed to cattle. As it is pollution-free and environmentally benign, using green resources for the biosynthesis of Fe<sub>3</sub>O<sub>4</sub>-NPs is preferable to chemical synthesis. According to the findings of this investigation, the leaves of *Alternanthera philoxeroides* are essential for the bioreduction and stability of iron (ii) (iii) ions to form Fe<sub>3</sub>O<sub>4</sub>-NPs. The nanoparticles' photocatalytic abilities were also assessed. Utilizing a variety of methods, including UV-visible, FT-IR, TGA, DTA, and VSM, the Fe<sub>3</sub>O<sub>4</sub>-NPs were characterized. The biomolecules involved in the reduction of iron ions and capping of the bioreduced Fe<sub>3</sub>O<sub>4</sub>-NPs created by the *Alternanthera Philoxeroides* extract were discovered using FT-IR spectra. Results from the UV-visible range revealed a maximum peak at a shorter wavelength (330 nm), indicating the presence of iron nanoparticles and pointing to a critical function for the extract solution's reducing chemicals in the transformation of iron ions into Fe<sub>3</sub>O<sub>4</sub>-NPs. The iron nanoparticles showed notable photocatalytic activity in dye breakdown and hold potential as a greener alternative to treating chemical waste water. This research reveals that the leaf extract of *Alternanthera philoxeroides* can operate as a natural reducing agent for the green production of Fe<sub>3</sub>O<sub>4</sub>-NPs with potential photocatalytic capabilities. Potential uses for these nanoparticles include the treatment of waste water and environmental cleanup. To completely grasp their safety and effectiveness in human applications, however, more research is required.

#### Acknowledgement

This research work has been done with the financial support of University Grants Commission fund through the Faculty of Engineering, University of Rajshahi, Bangladesh (2022-23). The researchers also

acknowledge the supports of GARE, BANBEIS, Ministry of Education, BANGLADESH under Nano and Biotechnology Lab University of Rajshahi, Bangladesh, Ministry of Science and Technology, Bangladesh, Bangladesh Atomic Energy Commission and Institute of Fuel Research and Development (IFRD), BCSIR, Dhaka. Declaration: All the authors do not have any possible conflicts of interest.

#### Reference

**Nam J, Won N, Jin H, Chung H, Kim S.** 2009. pH-induced aggregation of gold nanoparticles for photothermal cancer therapy. *Journal of the American Chemical Society* **131**, 13639–45.

**Narayanan KB, Sakthivel N.** 2011. Synthesis and characterization of nano-gold composite using *Cylindrocladium floridanum* and its heterogeneous catalysis in the degradation of 4-nitrophenol. *Journal of Hazardous Materials* **189**, 519–25.

**Li J, Chen X, Ai N, Hao J, Chen Q, Strauf S.** 2011. Silver nanoparticle doped TiO<sub>2</sub> nanofiber dye sensitized solar cells. *Chem Phys Lett* **514**, 141–5.

**Horwat D, Zakharov DI, Endrino JL, Soldera F, Anders A, Migot S.** 2011. Chemistry, phase formation, and catalytic activity of thin palladium-containing oxide films synthesized by plasma-assisted physical vapor deposition. *Surface and Coatings Technology* **205**, S171–7.

**Dillon AC, Mahan AH, Deshpande R, Alleman JL, Blackburn JL, Parillia PA.** 2006. Hot-wire chemical vapor synthesis for a variety of nano-materials with novel applications. *Thin Solid Films* **501**, 216–20.

**Sobhani M, Rezaie HR, Naghizadeh R.** 2008. Sol-gel synthesis of aluminum titanate (Al<sub>2</sub>TiO<sub>5</sub>) nano-particles. *Journal of Materials Processing Technology* **206**, 282–5.

**Nadagouda MN, Speth TF, Varma RS.** 2011. Microwave-assisted green synthesis of silver nanostructures. *Journal of Hazardous Materials* **44**, 469–78.



- Wani IA, Ganguly A, Ahmed J, Ahmad T.** 2011. Silver nanoparticles: ultrasonic wave assisted synthesis, optical characterization and surface area studies. *Mater Lett* **65**, 520–2.
- Starowicz M, Stypula B, Banas J.** 2006. Electrochemical synthesis of silver nanoparticles. *Electrochem Commun* **8**, 227–30.
- Balaji DS, Basavaraja S, Deshpandeb R, Mahesh DB, Prabhakara BK, Venkataraman A.** 2009. Extracellular biosynthesis of functionalized silver nanoparticles by strains of *Cladosporium cladosporioides* fungus. *Colloids Surf B: Biointerfaces* **68**, 88–92.
- Shahverdi AR, Minaeian S, Shahverdi HR, Jamalifar H, Nohi AA.** 2007. NRapid synthesis of silver nanoparticles using culture supernatants of Enterobacteria: a novel biological approach. *Process Biochem* **42**, 919–23.
- Kumar KP, Paul W, Sharma CP.** 2011. Green synthesis of gold nanoparticles with Zingiber officinale extract: characterization and blood compatibility. *Process Biochem* **46**, 2007–13.
- Dubey SP, Lahtinen M, Sillanpaa M.** 2010. Tansy fruit mediated greener synthesis of silver and gold nanoparticles. *Process Biochem* **45**, 1065–71.
- Sukirtha R, Priyanka KM, Antony JJ, Kamalakkannan S, Thangam R, Gunasekaran P.** 2012. Cytotoxic effect of Green synthesized silver nanoparticles using *Melia azedarach* against in vitro HeLa cell lines and lymphoma mice model. *Process Biochem* **47**, 273–9.
- Mohamed Saleh A.** 2017. "Immobilization of horseradish peroxidase on Fe<sub>3</sub>O<sub>4</sub> magnetic nanoparticles." *Electronic Journal of Biotechnology* **27**, 84-90.
- Hou Yanglong.** 2005. "Inorganic nanocrystal self-assembly via the inclusion interaction of  $\beta$ -cyclodextrins: toward 3D spherical magnetite." *The Journal of Physical Chemistry B* **109(11)**, 4845-4852.
- Jian Pan.** 2006. "Preparation of polysulfone–Fe<sub>3</sub>O<sub>4</sub> composite ultrafiltration membrane and its behavior in magnetic field." *Journal of Membrane Science* **284**, 1-2 9-16.
- Cain Jason L.** 1996. "Preparation of  $\alpha$ -Fe particles by reduction of ferrous ion in lecithin/cyclohexane/water association colloids." *Journal of magnetism and magnetic materials* **155(13)**, 67-69.
- Mondal K.** 2004. "Reduction of iron oxide in carbon monoxide atmosphere—reaction controlled kinetics." *Fuel Processing Technology* **86(1)**, 33-47.
- Basavegowda Nagaraj.** 2014. "Green fabrication of ferromagnetic Fe<sub>3</sub>O<sub>4</sub> nanoparticles and their novel catalytic applications for the synthesis of biologically interesting benzoxazinone and benzthioxazinone derivatives." *New Journal of Chemistry* **38(11)**, 5415-5420.
- Basavegowda Nagaraj, Kanchan Mishra, Yong Rok Lee.** 2014. "Sonochemically synthesized ferromagnetic Fe<sub>3</sub>O<sub>4</sub> nanoparticles as a recyclable catalyst for the preparation of pyrrolo [3, 4-c] quinoline-1, 3-dione derivatives." *RSC Advances* **106(4)**, 61660-61666.
- Senthil M, Ramesh C.** 2012. "BIOGENIC SYNTHESIS OF Fe<sub>3</sub>O<sub>4</sub> NANOPARTICLES USING TRIDAX PROCUMBENS LEAF EXTRACT AND ITS ANTIBACTERIAL ACTIVITY ON PSEUDOMONAS AERUGINOSA." *Digest Journal of Nanomaterials & Biostructures (DJNB)* **7(4)**.
- Latha N, Gowri M.** 2014. "Biosynthesis and characterisation of Fe<sub>3</sub>O<sub>4</sub> nanoparticles using *Caricaya papaya* leaves extract." *International Journal of Scientific and Research* **3(11)**, 1551-1556.
- Venkateswarlu Sada.** 2013. "Biogenic synthesis of Fe<sub>3</sub>O<sub>4</sub> magnetic nanoparticles using plantain peel extract." *Materials Letters* **100**, 241-244.
- Narayanan Sreeja.** 2012. "Biocompatible magnetite/gold nanohybrid contrast agents via green chemistry for MRI and CT bioimaging." *ACS applied materials & interfaces* **4(1)**, 251-260.

- Venkateswarlu Sada.** 2014. "Bio-inspired green synthesis of Fe<sub>3</sub>O<sub>4</sub> spherical magnetic nanoparticles using *Syzygium cumini* seed extract." *Physica B: Condensed Matter* **449**, 67-71.
- Pham Xuan Nui.** 2016. "Synthesis and characterization of chitosan-coated magnetite nanoparticles and their application in curcumin drug delivery." *Advances in Natural Sciences: Nanoscience and Nanotechnology* **7(4)**, 045010.
- Ramesh AV.** 2018. "Facile green synthesis of Fe<sub>3</sub>O<sub>4</sub> nanoparticles using aqueous leaf extract of *Zanthoxylum armatum* DC. for efficient adsorption of methylene blue." *Journal of Asian Ceramic Societies* **6(2)**, 145-155.
- Ahmad Sharif.** 2009. "Soft template synthesis of super paramagnetic Fe<sub>3</sub>O<sub>4</sub> nanoparticles a novel technique." *Journal of Inorganic and Organometallic Polymers and Materials* **19**, 355-360.
- Bishnoi, Shahana, Aarti Kumar, Raja Selvaraj.** 2018. "Facile synthesis of magnetic iron oxide nanoparticles using inedible *Cynometra ramiflora* fruit extract waste and their photocatalytic degradation of methylene blue dye." *Materials Research Bulletin* **97**, 121-127.
- Yew Yen Pin.** 2016. "Green synthesis of magnetite (Fe<sub>3</sub>O<sub>4</sub>) nanoparticles using seaweed (*Kappaphycus alvarezii*) extract." *Nanoscale research letters* **11**, 1-7.
- Sirdeshpande, Karthikey Devadatta,** 2018. "Structural characterization of mesoporous magnetite nanoparticles synthesized using the leaf extract of *Calliandra haematocephala* and their photocatalytic degradation of malachite green dye." *Applied Nanoscience* **8**, 675-683.
- Ahmad Sharif.** 2009. "Soft template synthesis of super paramagnetic Fe<sub>3</sub>O<sub>4</sub> nanoparticles a novel technique." *Journal of Inorganic and Organometallic Polymers and Materials* **19**, 355-360.
- Das Chanchal.** 2020. "Green synthesis, characterization and application of natural product coated magnetite nanoparticles for wastewater treatment." *Nanomaterials* **10(8)**, 1615.
- Pham Xuan Nui.** 2016. "Synthesis and characterization of chitosan-coated magnetite nanoparticles and their application in curcumin drug delivery." *Advances in Natural Sciences: Nanoscience and Nanotechnology* **7(4)**, 045010.
- Akbarizadeh, Majid Reza.** 2022. "Cytotoxic activity and Magnetic Behavior of green synthesized iron oxide nanoparticles on brain glioblastoma cells." *Nanomedicine Research Journal* **7(1)**, 99-106.
- Rami JM.** 2021. "Thermogravimetric analysis (TGA) of some synthesized metal oxide nanoparticles." *Materials Today: Proceedings* **43**, 655-659.
- Bhuiyan Md Shakhawat Hossen.** 2020. "Green synthesis of iron oxide nanoparticle using *Carica papaya* leaf extract: application for photocatalytic degradation of remazol yellow RR dye and antibacterial activity." *Heliyon* **6(8)**.
- Rajendrachari, Shashanka.** 2020. "A fast and robust approach for the green synthesis of spherical Magnetite (Fe<sub>3</sub>O<sub>4</sub>) nanoparticles by *Tilia Tomentosa* (Ihlamur) leaves and its antibacterial studies.
- Jalil WBF.** 2017. "Low toxicity superparamagnetic magnetite nanoparticles: One-pot facile green synthesis for biological applications." *Materials Science and Engineering: C* **78**, 457-466.